Andrographis paniculata Mediated AuNPs as Anti-Microbial, Antioxidant, Anti-Diabetic Agents and their Efficacy in Wound Healing of Mice

Can Wu [a,b] and Liang Huang [a,b,*]

* *Corresponding author: qkyf666@smu.edu.cn*

DOI: 10.15376/biores.20.2.2687-2710

GRAPHICAL ABSTRACT

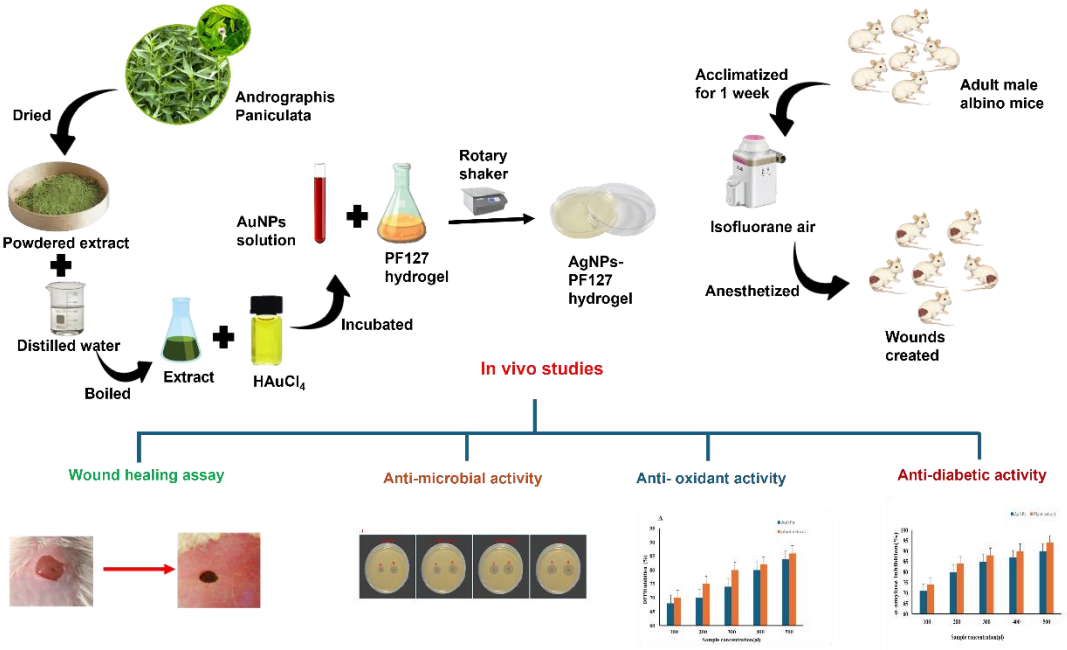

Andrographis paniculata Mediated AuNPs as Anti-Microbial, Antioxidant, Anti-Diabetic Agents and their Efficacy in Wound Healing of Mice

Can Wu [a,b] and Liang Huang [a,b,*]

Gold nanoparticles (AuNPs) are known to have low toxicity and biocompatibility. Meanwhile, *Andrographis paniculata* (*A. paniculata*) is a medicinal plant known for its therapeutic benefits. Traditional methods for the synthesis of AuNPs frequently depend on toxic compounds, which present environmental and health hazards. In this work, *A. paniculata* was combined with AuNPs to enhance its antimicrobial, antioxidant, and wound healing effects, thereby offering a safer and more effective alternative compared to current available methods. Water-soluble gold metal ions were reduced to neutral metal nanoparticles in the course of reaction with aqueous *A. paniculata* extract. The biosynthesised AuNPs was examined using UV-Vis, FTIR Spectroscopy, TEM, XRD, SAED Diffraction, EDX, DLS, and zeta potential measurements. AuNPs were incorporated into nonionic surfactant to form a thick, readily spreadable hydrogel. The mixture was found to enhance the wound contraction rate with no skin irritation observed in treated mice. The study demonstrated a simple and environmentally safe approach to produce AuNPs with improved antimicrobial, antioxidant, antidiabetic and wound healing abilities. The AuNPs-PF127 hydrogel is a non-toxic and bio-friendly delivery technology that shows potential in promoting healing of wounds, burns, *etc*.

DOI: 10.15376/biores.20.2.2687-2710

Keywords: Gold nanoparticles; Wound healing; Antioxidant; Anti-diabetic; Anti-microbial; Hydrogel; Andrographis paniculata

Contact information: a: Clinical Pharmacy Centre, Nan fang Hospital, Southern Medical University, Guangzhou 510515, Guangdong, China, b: Department of pharmacy, Nan fang Hospital, Southern Medical University, Guangzhou 510515, Guangdong, China;
** Corresponding author: qkyf666@smu.edu.cn*

INTRODUCTION

The trend towards producing metal nanoparticles through a sustainable and eco-friendly method is increasing, with the goal of reducing negative effects in therapeutic and medical applications (Elahi *et al.* 2018; Kalimuthu *et al.* 2020; Lee *et al*. 2020). Biological pathways utilizing plants and microorganisms offer a safer alternative compared to traditional chemical synthesis processes that could potentially have environmental and health hazards. Biological approaches are frequently used in targeted drug delivery, medical imaging, sensing, and photothermal therapy. Plant-mediated biosynthesis utilizes phytochemicals to create nanoparticles with improved anti-diabetic, antioxidant, antibacterial and wound healing effects. Various metals have been converted into nanoparticles by interacting with organic components present in plant materials (Siddiqi *et al.* 2017; Bapat *et al.* 2020; Patil *et al.* 2020; Qiao and Qi 2021). This technique utilizes the abundant phytochemicals in plants to help reduce metal ions into nanoparticles. Plant-based synthesis provides a sustainable method for producing nanoparticles and imparts biological activity to the nanoparticles due to their phytochemical origins.

Gold nanoparticles (AuNPs) have a significant background in applications such as bioimaging and medication delivery systems. AuNPs have unique physicochemical and photothermal characteristics that enable precise administration and dispersion of customized medications to specific cells or tissues. AuNPs are distinguished by their surface plasmon resonance (SPR) and distinctive optical properties, which have been utilized in creating advanced therapeutic and diagnostic instruments. Metal nanoparticles, such as AuNPs, are synthesized biologically, providing benefits of compatibility with living organisms and eco-friendliness, which are very desirable for medicinal uses. Recently, the use of AuNPs in imaging and medicinal fields has grown due to their flexible features and ability to improve the effectiveness and specificity of treatment methods. AuNPs are valued for their chemical stability, efficiency in absorbing infrared radiation, simple manufacturing, and their ability to improve wound healing processes (Niska *et al.* 2018). AuNPs act by directly interacting with bacterial cell walls and binding to bacterial DNA, which hinders the unwinding of the double helix necessary for replication or transcription. This dual action has both bactericidal and bacteriostatic effects, allowing for the targeting of antibiotic-resistant organisms including *P. aeruginosa* and *S. aureus*. AuNPs have the ability inhibit the production of reactive oxygen species (ROS), thereby acting as powerful antioxidants and enhancing the process of wound healing (Vijayakumar *et al*. 2019).

Thermo-sensitive hydrogels are highly favoured materials in drug delivery systems for wound healing process. These hydrogels are praised for their capacity to hold water, evenly distribute therapeutic chemicals, and able to their regulate substance or compound release (Huang *et al*. 2019). At body temperature the thermo-reversible PF-127 undergoes a sol-gel transition and has demonstrated potential for improving the healing of topical wounds (Arafa *et al*. 2018).

Traditional medicinal plants are being evaluated as potential sources of innovative pharmaceuticals to combat antibiotic-resistant bacteria (Anand *et al* 2019). *Andrographis paniculata* (*A. paniculata*), also called green chiretta, is well-known in traditional medicine in China, India, and Southeast Asia for its effectiveness in treating fever, snake bites, diarrhoea, infections, wounds, and itchiness (Kumar *et al.* 2004; Akbar 2011; Chen *et al.* 2014; Kabir *et al.* 2014). Various therapeutic properties of *A. paniculata* extracts are acknowledged, such as anti-inflammatory (Sheeja *et al.* 2006), antioxidant (Tripathi and Kamat 2007), antiviral (Calabrese *et al.* 2000), anticancer (Ajaya *et al.* 2004), and antimicrobial effects (Singha *et al.* 2003). *A. paniculata* is mostly identified for its antioxidant activity (Trivedi and Rawal 2001), which is essential for the protection of tissues from oxidative damage and the enhancement of wound healing (Martin 1996). The wound-healing efficacy of *A. paniculata* leaf extract is further confirmed by its antimicrobial activity (Singha *et al.* 2003), which may be accomplished through promoting antioxidant production at the wound site and establishing a favourable environment for tissue repair (Shukla *et al.* 1999). Applying a 10% aqueous leaf extract of *A. paniculata* can greatly enhance wound healing in rats. It reduces inflammation, decreased scarring, increased development of new blood vessels, and promotes higher levels of collagen in the healed tissue (Al-Bayaty *et al.* 2012).

In this study, the leaves of the *A. paniculata* plant were used to create AuNPs. The wound healing, anti-diabetic, anti-bacterial, and antioxidant properties of the AuNPs produced through biosynthesis are extensively studied through diverse characterization techniques. The thermo-sensitive and hydrophilic polymer PF127 was used as a safe and biocompatible hydrogel to distribute AuNPs in a topical formulation on mouse skin to enhance wound healing.

EXPERIMENTAL

The compound Tetrachloroauric acid ($HAuCl_4$) and other necessary substances were obtained from Sigma-Aldrich (Shanghai, China). All glassware used in the study was cleaned carefully with distilled water to maintain cleanliness and reduce the risk of contamination before starting the experimental procedures.

Collection and Preparation of Plant Extract

Leaves of *A. paniculata* were dried in shade for 15 days post-collection in a darkened chamber and then pulverized into a fine powder. In an Erlenmeyer flask, 100 mL of distilled water was combined with 10 g of powdered leaf and heated for 20 min until it reached 50 °C. The mixture was filtered using Whatman filter paper no. 1 and stored at 4 °C.

Biosynthesis of AuNPs

Synthesis of AuNPs was carried on following the method of Ghosh *et al.* (2012) A total of 1 mL of *A. paniculata's* aqueous leaf extract was mixed with 9 mL of a 1.0 mM $HAuCl_4$ solution. The combination was permitted to react under static conditions in a dark room for 24 h. The production of AuNPs was verified through colour shift, signifying the synthesis of AuNPs.

Characterisation

The production of AuNPs using *A. paniculata* leaf extract and $HAuCl_4$ solution was analysed by measuring the absorbance spectrum with UV-Vis spectroscopy from 400 to 700 nm. The zeta potential and hydrodynamic size of the produced AuNPs were evaluated using DLS techniques at 25 °C. TEM was used to analyse the size, shape, and morphological characteristics of the AuNPs produced using the *A. paniculata* leaf extract. FTIR was used to determine functional groups and surface chemical residues on the AuNPs. This investigation aimed to verify the total reduction of Au^{3+} ions by the *A. paniculata* leaf extract. The Rigaku Mini Flex was used for XRD examination for a thorough analysis of the crystalline structure of the generated AuNPs. EDX was conducted using a JEM 2100F equipment, operating at 200 kV.

Antioxidant Assay

DPPH (2,2-diphenyl-1-picrylhydrazyl) Assay

This method was used to assess the antioxidant capacity of the produced AuNPs and aqueous plant extract. The extract and nanoparticles were combined completely and incubated in darkness for 30 min at room temperature. The samples absorbance was measured at 517 nm after adding 1.5 mL of 0.1 mM DPPH solution and adjusting the total volume to 2 mL in the test tube with sterile distilled water. The linear regression value was determined using ascorbic acid as standard (Nurhaslina *et al.* 2019). The DPPH radical scavenging activity percentage was calculated using Eq. 1.

$$\% \text{ of RSA} = [A(\text{control}) - B(\text{sample}) / A(\text{control})] \times 100 \quad (1)$$

Anti-Microbial Assay

Bacterial strains such as *P. aeruginosa*, *S. aureus*, *S. pneumoniae*, and *E. coli* were used in the antimicrobial research. The cultures were preserved as glycerol stocks at -80 °C and were reactivated from the glycerol stock for subculturing in nutrient broth kept at 4 °C. The effectiveness of the produced AuNPs against bacteria was assessed using the agar well diffusion method (Kifle and Enyew 2022). Evenly distributed bacterial suspensions were applied onto nutrient agar plates, which were subsequently punctured to form wells with a cork borer. AuNPs solution of 100 µL was added to

each well, and the plates were incubated for 24 h at 37 °C. Amoxicillin served as the reference antibiotic, and the antibacterial effectiveness was assessed by measuring the size of the zones of inhibition surrounding the wells.

Anti-Diabetic Assay

α-Amylase Inhibition Assay

The α-amylase inhibition experiment, which assesses anti-diabetic potential, was performed using the 3,5-dinitrosalicylic acid (DNS) method (Al-Dahmash 2021). AuNPs and plant extracts were produced in PBS ranging from 100 to 500 mg/mL concentrations for this experiment. A 200 units/mL concentration of α-amylase was combined with different amounts of a starch solution and left to incubate for 3 min. By adding 200 µL of DNS reagent and heating of mixture for 10 min at 85 °C will terminate the reaction. After the reaction, 5 mL of distilled water was used to thin the liquid, and absorbance was measured at 540 nm. Blanks were created by substituting the test materials with buffer of equivalent amounts to set a standard for enzyme activity. Sample blanks were generated without the enzyme solution for each concentration to compensate for any natural absorbance of the materials. Acarbose, an established antidiabetic medication, was used as the positive control in the assay, which was performed in the same manner as the test samples. The inhibition of α-amylase was measured as follows,

$$\text{Inhibition \%} = [(A_c\text{-}A_{cb}) \times (A_s\text{-}A_{sb}) / (A_c\text{-}A_{cb})] \times 100 \quad (2)$$

where, A_s is the absorbance of sample, A_c is the absorbance of control, A_{sb} is the absorbance of sample's blank, and A_{cb} is the absorbance of control's blank.

Wound Healing Assay

Synthesis of AuNPs-PF127 hydrogel

A 30% w/v PF-127 hydrogel (PF127) was created using ice-cold PBS. Three different concentrations of AuNPs (0.3, 1.0, and 3.0 mg) were added to the PF127 hydrogel to create the treatment hydrogels. The mixtures were stirred overnight on a rotary shaker in a cold environment to achieve a consistent solution. The hydrogels were stored at 4 °C.

Assessment of the physicochemical characteristics of AuNPs-PF127 hydrogel

The physical features of the PF127 base hydrogel and the AuNPs-infused treatment hydrogels were visually evaluated for attributes such consistency, homogeneity, and colour. The pH of the hydrogels was measured with a standard pH metre after they were diluted to a 1% concentration with distilled water. The viscosity of the hydrogels was measured using an Ostwald viscometer kept at 4 °C. The spreading ability of the hydrogel was assessed by applying 50 µL between two glass slides and leaving it for 10 min without interruption (El-Houssieny *et al.* 2010). The diameter of the hydrogel spread was measured to assess its spreading ability.

Rheology investigations of AuNPs-PF127 hydrogel

The rheological properties were analysed using a rheometer (Physica MCR 92, Anton Paar, Germany). A temperature sweep test was conducted at a constant frequency of 1 Hz with a gap size of 0.5 mm, gradually increasing the temperature from 5 to 45 °C at a rate of 1 °C/min. The PF127 hydrogel and the AuNPs-PF127 hydrogel were both subjected to temperature fluctuations, and the storage modulus (+Ve) and loss modulus (-Ve) were recorded. The gelation temperature was determined by examining the intersection of the values of (+Ve) and (-Ve).

Skin irritation test

The assessment of potential skin irritation from the hydrogel treatment on mice was carried out using the approach outlined by (Mohamad *et al.* 2014). Pristine PF127 hydrogel of 20 µL and 3 mg AuNPs-PF127 hydrogel were applied to the shaved back skin of the mice. Skin reactions were observed and recorded at 1, 6, 24, and 48 h after treatment.

In vivo experiment on wound healing

Adult male albino mice, weighing 25 to 30 g and pathogen free, were housed in a controlled environment with a 12-h light/dark cycle. The mice were provided with regular mouse food and purified water throughout the experiment. After one week of acclimatisation period, the mice were anaesthetized using a 5% v/v isoflurane/air mixture, which was reduced and maintained at 2.5% v/v during the procedure. The back skin was shaved and disinfected with 70% ethyl alcohol. A circular wound with a diameter of 6 mm was created, going through all skin layers. The mice were divided into four groups of six: Group I served as the control; Group II received PF127 hydrogel; Group III was treated with 0.3 mg AuNPs-PF127 hydrogel; and Group IV was treated with 1.0 mg AuNPs-PF127 hydrogel. A 20 µL hydrogel sample was applied to the wound area on Day 1, then covered with Tegaderm and Opsite Flexifix transparent dressing. The wound healing process was monitored on Days 3,5,7, 10 post-surgery. Ethical requirements have been met with regards to the humane treatment of animals described in the study and the study received approval from the Institutional Review Board of the Clinical Pharmacy Centre, Southern Medical University.

The percentage of wound contraction was determined by Eq. 3.

$$\text{Wound contraction (\%)} = (\text{Wound area day 1} - \text{Wound area day n}) / \text{Wound area day 1} \times 100 \quad (3)$$

Statistical Analysis

The results are expressed as Mean ± Standard Deviation. 10th version SPSS software is used to perform all the statistical analyses. Analysis was done in triplicate, and the mean was used for statistical analysis. One-way ANOVA test was used determination of statistical significance, succeeded by post hoc Tukey test. $P < 0.05$. was the fixed statistical significance.

RESULTS AND DISCUSSION

Synthesis of AuNPs

The effectiveness of biosynthesized AuNPs depends on fine-tuning preparation parameters such pH, temperature, plant extract content, and $HAuCl_4$ concentration. By precisely optimising these parameters, it is feasible to synthesize AuNPs with specific shapes, topologies, and size distributions designed for wound healing applications, as shown in Table 1. The colour change from pale yellow to ruby red was observed over five days after combining the aqueous *A. paniculata* extract with $HAuCl_4$ solutions indicating the successful synthesis of AuNPs, as shown in Fig. 1. The colour shift serves as a visual indicator of nanoparticles synthesis, highlighting the distinctive characteristics of AuNPs for medicinal and therapeutic uses.

Table. 1. Optimising Parameters to Prepare the AuNPs

Parameter	Optimising Parameter
Plant extract	1.5 mL
$HAuCl_4$ concentration	0.5 mM
Temperature and Reaction time	60 ℃, 30 min
pH	6

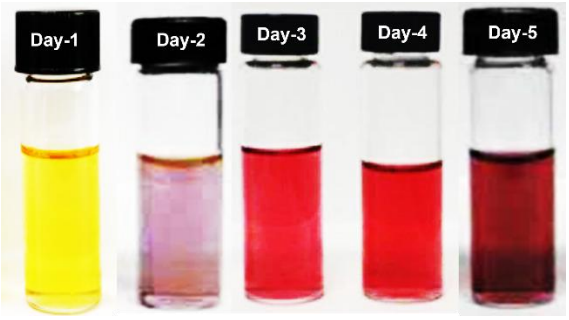

Fig. 1. Colour change observed during formation of AuNPs using *A. paniculata* extract

Characterisation

UV-Visible spectroscopy

The UV-Vis spectra of AuNPs are influenced by various parameters such as nanoparticle size, shape, and concentration (Guo *et al.* 2015). The typical SPR of gold occurs within the wavelength range of 500 to 550 nm (Siddiqi *et al.* 2018). The UV-Vis spectra showed the presence of the SPR band of the AuNPs at around 540 nm (Fig. 2). This aligns with prior studies (Arunachalam *et al.* 2013; Nyabola *et al.* 2020).

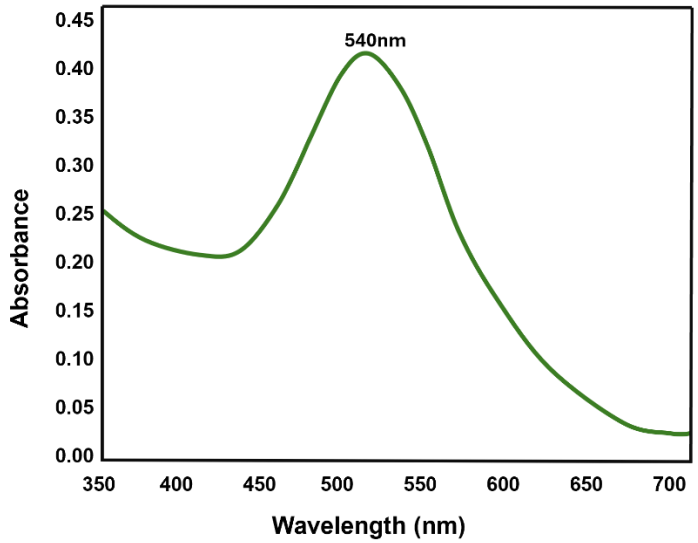

Fig. 2. UV spectra of AuNPs synthesised using *A. paniculata* extract

FTIR spectroscopy

The functional groups in *A. paniculata* extract, which may facilitate the stabilization of AuNPs and the reduction of Au^{3+} ions, were identified through FTIR spectroscopy. Significant bioactive molecules found in *A. paniculata* are terpenoids, alkaloids, saponins, and flavonoids. Characteristic bands are shown in the FTIR spectra (Fig. 3) of both the synthesised AuNPs and plant extract. The O–H and C–H stretching vibrations of the *A. paniculata* extract are recorded at 3426 and 2921 cm^{-1} respectively (Dao *et al.* 2021). A prominent absorption band at 1030 cm^{-1} also corresponds with the

–C–O vibrational group; C=C and C=O stretching in aromatic compounds provides the peak at 1620 cm^{-1}. However, the synthesized AuNPs exhibited distinct peaks at 3474.43 (–OH), 2012.23 (–C–H), 1640 (C=O stretching). Also, the other bands found at 1530.11, and 750.34 cm^{-1} corresponded to fatty acid groups. The observed shifts in absorbance wavelengths and the disappearance of several peaks imply that the *A. paniculata* extract comprises necessary secondary metabolites able to function as capping and reducing agents during AuNP synthesis. These variations in functional group peaks highlight the part the extract works in stabilising and reducing the produced nanoparticles. These groups also have wound healing and antibacterial action. Hydroxyl group compounds such as phenols and polyphenols can mess with cell membranes and stop bacterial growth. In particular, medium-chain fatty acids, such as lauric acid, have shown antibacterial action against many kinds of infections.

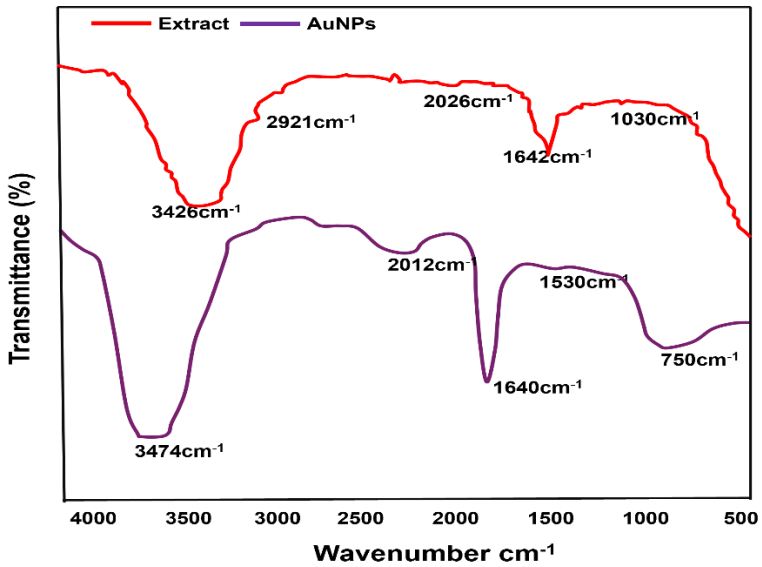

Fig. 3. FTIR spectra of AuNPs bio fabricated using Aqueous leaf extract of *A. paniculata*

Transmission electron microscopy

The TEM analysis concentrated on the shape and size of nanoparticles. Figure 4 shows that the AuNPs were mostly between 20 to 30 nm in size, and the images highlighted the spherical shape of most the nanoparticles. Earlier studies have shown that AuNPs produced by marine microorganisms are normally between 50 and 100 nm in size (Shanmugam *et al.* 2020). The results also indicate that the particle size of AuNPs in this study was smaller than those synthesized by using the marine microorganisms (~50 nm), which affirms the excellent role of biomolecules in the *A. paniculata* extract as reducing and stabilizing agents for the preparation of AuNPs. Smaller nanoparticles might have a larger surface area to interact with microbial cells or free radicals, enhancing their effectiveness (Rajakannu *et al* 2015; Gupta S *et al* 2024)

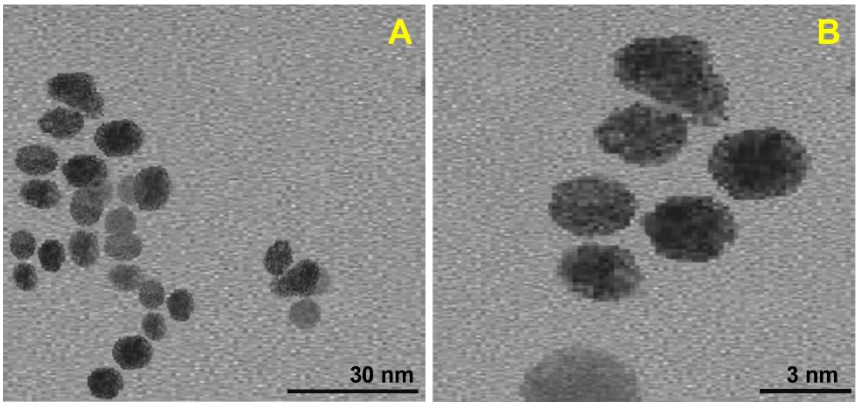

Fig. 4. TEM images of biosynthesised AuNPs using *A. paniculata*

Scanning Electron Diffraction (SAED) analysis

SAED analysis is essential for the identification of the crystallographic structure of nanoparticles. The polycrystalline nature of the particles was confirmed by the presence of concentric rings in the diffraction pattern (as shown in Fig. 5). The crystal structure of AuNPs was determined by both SAED and XRD (Fig. 6.) with each technique providing unique insights. SAED provided diffraction patterns that revealed the crystallographic structure and structural properties of the AuNPs, complementing the TEM results. Together, SAED and TEM provided a comprehensive understanding of the nanoparticles' structure.

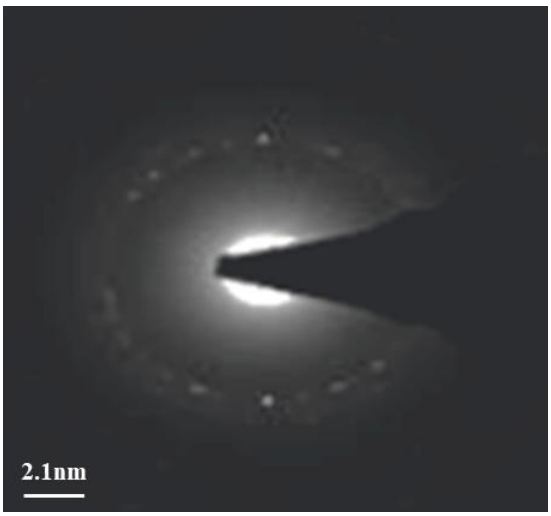

Fig. 5. SAED pattern of biosynthesised AuNPs

X-Ray diffraction studies

XRD patterns of AuNPs displayed diffraction peaks at 2θ angles of 27.21°, 33.44°, 56.61°, and 73.63° within a scanning range of 10° to 80° (Fig. 6). The peaks represent the crystal planes (111), (200), (220), and (311) of AuNPs, verifying their cubic symmetry as per the JCPDS database file 04-0784. D-spacing values associated with these planes were also recorded (Fig. 6). Furthermore, the amorphous phases of organic compounds that surround the crystalline AuNPs may be indicated by a broad peak at 27°, a phenomenon that has been previously observed (Nguyen *et al.* 2022). In addition, the (111) peak's intensity is considerably greater than that of other signals, suggesting that the (111) plane is the primary growth direction during the crystallisation of AuNPs (Owaid *et al.* 2019).

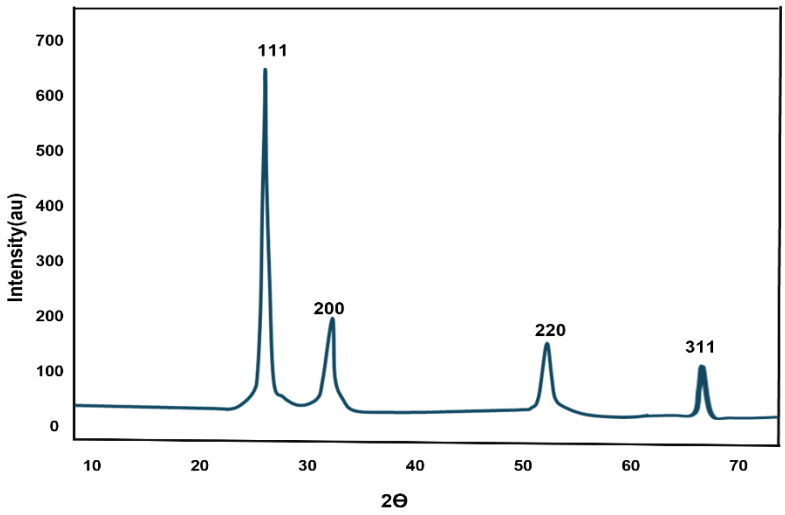

Fig. 6. XRD pattern of AuNPs

Energy dispersive X-Ray analysis

The EDX examination of AuNPs revealed an optical absorption peak at around 2.2 keV, which is characteristic of metallic AuNPs, with two additional minor peaks at 8.5 and 9.7 keV, respectively (Fig. 7). The results of this analysis confirm that gold was the primary element, accounting for 48.6% of the total weight (Elavazhagan and Arunachalam 2011). The presence of metallic gold and SPR band obtained from UV-Vis analysis along with XRD results further confirmed the formation of AuNPs using A. paniculata extract.

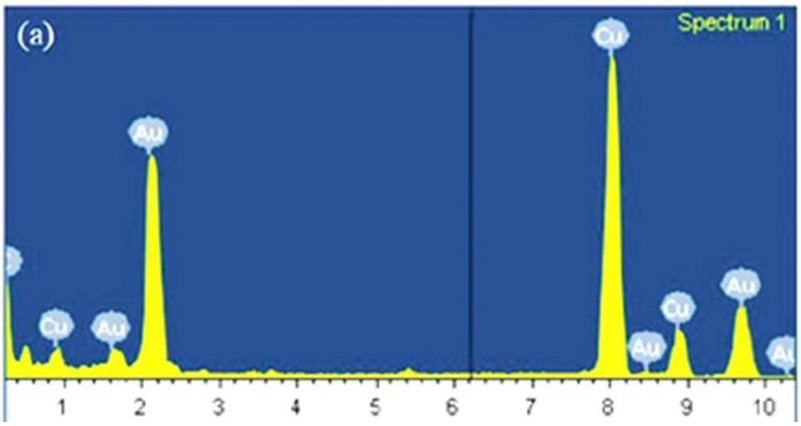

Fig. 7. EDX pattern of AuNPs

Dynamic light scattering

The particle size distribution of the AuNPs was evaluated by DLS, which revealed a main size distribution centered at about 23 nm Fig .8A. (Allafchian *et al.* 2022). Because of hydrodynamic radius examined with DLS, the synthetic AuNPs particle size value obtained in DLS technique is similar in comparison with TEM microscopic techniques, as shown in Fig. 4, signifying the successful formation of AuNPs on the nanoscale. This can be ascribed to the presence of secondary metabolites such as polyphenols, flavonoids, alkaloids, and triterpenoids, forming a stabilizing surface and preventing the aggregation of generated nanoparticles.

Furthermore, the zeta potential of biosynthesized AuNPs was approximately −25.7 mv. As shown in Fig. 8B, the surface potential of the AuNPs was evaluated through zeta potential measurements. In general, the stabilising agents that are produced during the synthesis and growth of AuNPs are responsible for the negative surface

charge of the material. In metal nanoparticles that are synthesised using plant extracts as reducing agents, negative zeta potentials are frequently observed. The stability of the colloidal system is suggested by the negative surface charge, which is the result of static repulsive interactions that were achieved through the green synthesis process of AuNPs (Unayana *et al.* 2020).

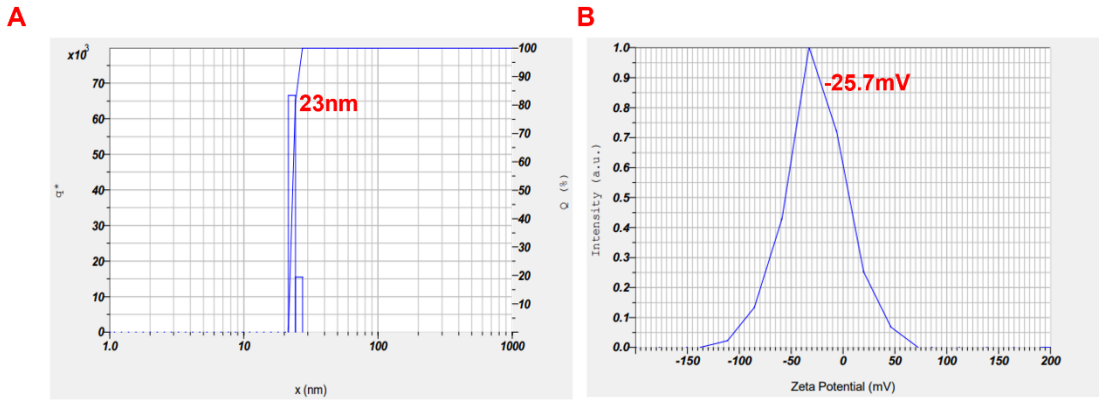

Fig. 8. DLS (A) and Zeta potential (B) of AuNPs

Evaluation of Antioxidant Activity

Phytochemical substances were evaluated to determine their antioxidant capacity using spectrometric analysis using the DPPH free radical scavenging technique. The study examined how biosynthesised AuNPs and the aqueous extract of *A. paniculata* can counteract DPPH radicals at different doses. The synthesised AuNPs at higher concentrations led to a significant increase in DPPH radical scavenging activity, as shown in Fig. 9. Both the plant extract and AuNPs demonstrated peak radical scavenging efficiencies ranging from 86% to 90% (v/v), and these results were statistically significant. The increased surface area and catalytic capabilities of the AuNPs probably played a role in their strong antioxidant effects. The excellent antioxidant behaviour of the extract can be attributed to the presence of flavonoids and phenolic compounds, in which the latter is well-known for exhibiting high activity, particularly against free radicals and nitric oxides (Benabderrahim *et al* 2019). The *A. paniculata* extract and biosynthesized AuNPs were found to be strong antioxidants according to the DPPH assay results.

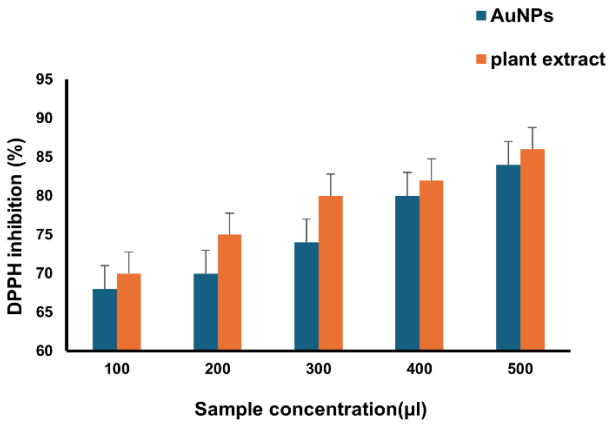

Fig. 9. Antioxidant activity of AuNPs synthesized using *A. paniculata*

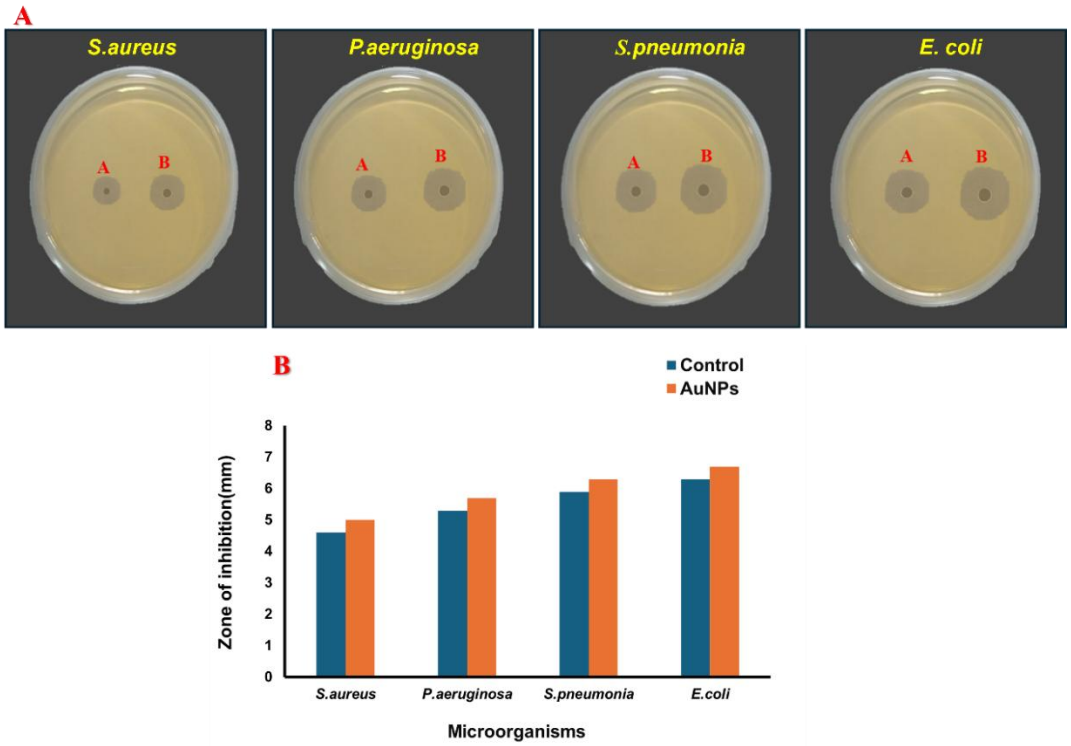

Fig. 10. Antimicrobial activity of AuNPs synthesized using *A. paniculata*. (A) Agar plates showing zones of inhibition; (B) diameter of zones of inhibition

Assessment of Antimicrobial Activity

The antimicrobial properties of the produced AuNPs were evaluated using the agar well diffusion method. The AuNPs solution was added to an agar well and left to incubate for 12 h. Amoxicillin (β-lactam antibiotic) was used as the positive control, as shown in Fig. 10A. The effectiveness was assessed by measuring the zone of inhibition surrounding the well after incubation. The nanoparticles produced using *A. paniculata* extracts had strong antibacterial characteristics, making them potential carriers for antibacterial agents, as outlined in Fig. 10B. The antimicrobial efficacy of AuNPs is highly dependent on the phytochemicals present in the plant extracts used for their synthesis. Each plant extract imparts unique properties to the AuNPs, making them suitable for different applications showed in Table 2.

Table 2. Synthesis of AuNPs from Different Plant Extracts and their Antimicrobial Activity

S. no.	Name of plant extract synthesizing AuNPs	Antimicrobial mechanism	Compounds	Applications	References
1	*Clove extract*	Disruption of Microbial Cell Walls	Eugenol	1. Oral Health 2. Medicinal uses 3. Food preservations 4. Cosmetic Products	(Mehrishi *et al.* 2020)
2	*Turmeric Extract*	Generation of Reactive Oxygen Species (ROS)	Curcumin	Broad-spectrum antibacterial applications in cosmetics and health supplements.	(Raymond *et al.* 2024)

3	*Garcinia kola*	Interaction with Microbial Enzymes	Phenolic compounds	Effective against foodborne pathogens and in wound care	(Akintelu *et al.* 2021)
4	*Vitex negundo*	DNA Damage	Flavonoids	traditional medicine for treating infections and inflammatory conditions.	(Shanwaz *et al.* 2023)
5	*A. paniculata*	a. Disruption of Microbial Cell Walls b. Generation of Reactive Oxygen Species (ROS) c. Interaction with Microbial Enzymes d. DNA Damage	Flavonoids and Polyphenols Antioxidants Bioactive compounds Phytochemicals	1. Wound healing 2. Antimicrobial Coatings 3. Antioxidant activity	Present work

Assessment of Anti-Diabetic Activity

The anti-diabetic properties of *A. paniculata* aqueous extract and biosynthesized AuNPs were assessed by an α-amylase inhibition experiment (Fig. 11). The aqueous extract and the biosynthesized AuNPs both showed a substantial ability to block α-amylase enzyme activity, indicating a noteworthy anti-diabetic impact of 90 to 93% (v/v). The strong amylase inhibitory action of the AuNPs can be attributed to the presence of phytochemicals such flavonoids and polyphenols, as shown by phytochemical screens and FTIR analysis. AuNPs from the *A. paniculata* plant showed strong antioxidant characteristics, which improved their ability to combat diabetes by lowering oxidative stress and blocking glucose hydrolyzing enzymes (Chen *et al* 2012; Batool *et al.* 2022). This work emphasizes the potential antioxidant and anti-diabetic properties of the aqueous extract of *A. paniculata* and phyto-generated AuNPs. It suggests that these substances could be used in natural-based treatment approaches for managing diabetes.

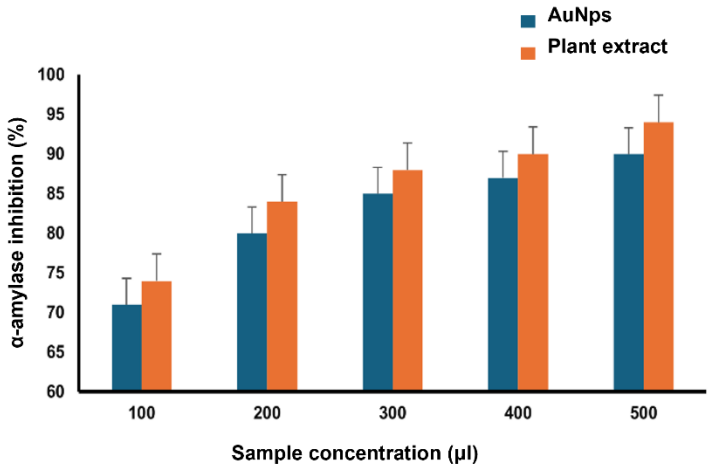

Fig. 11. Anti-diabetic activity of AuNPs synthesized using *A. paniculata*

Assessment of Wound Healing

Evaluation of AuNPs-PF127 Hydrogel and rheology studies

Adding AuNPs to the PF127 hydrogel caused it to turn pale red, unlike the original translucent PF127 hydrogel (Fig.12).

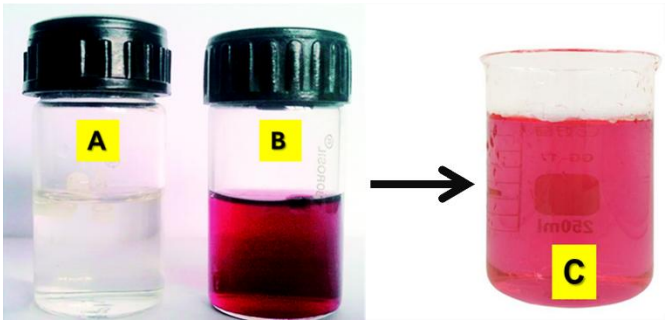

Fig. 12. (A) PF127 hydrogel (B) AuNPs (C) AuNPs-PF127 Hydrogel

Both hydrogels maintained a pH range of 5.7 to 5.8 and exhibited significant sol-gel transition characteristics, changing from a liquid state at 4 °C to a hydrogel state at 37 °C, within the temperature range of 22 to 37 °C. The hydrogels exhibited a temperature-dependent rise in viscosity and had a spreading ability ranging from 6.0 to 7.7 cm (Fig.13). Apart from the colour variation, the AuNPs-PF127 hydrogel retained the basic features of the PF127 base.

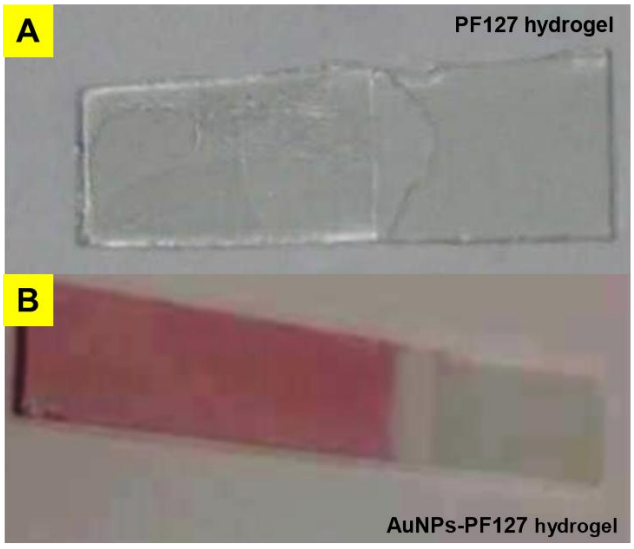

Fig. 13. (A) PF127 hydrogel (C) AuNPs-PF127 Hydrogel spreading ability images

Figures 14A and 14B illustrate the (+Ve) and (-Ve) values of PF127 hydrogel and AuNPs-PF127 hydrogel over a temperature range of 5 to 45 °C. Gelation temperature is defined as the point at which (+Ve) equals (-Ve) and the liquid transitions to a non-flowing gel. The plain hydrogel and the AuNPs-PF127 hydrogel were found to have gelation temperatures of 22.8 °C and 36.4 °C, respectively. The incorporation of AuNPs did not significantly influence the hydrogel's gelation capacity, as indicated by these results.

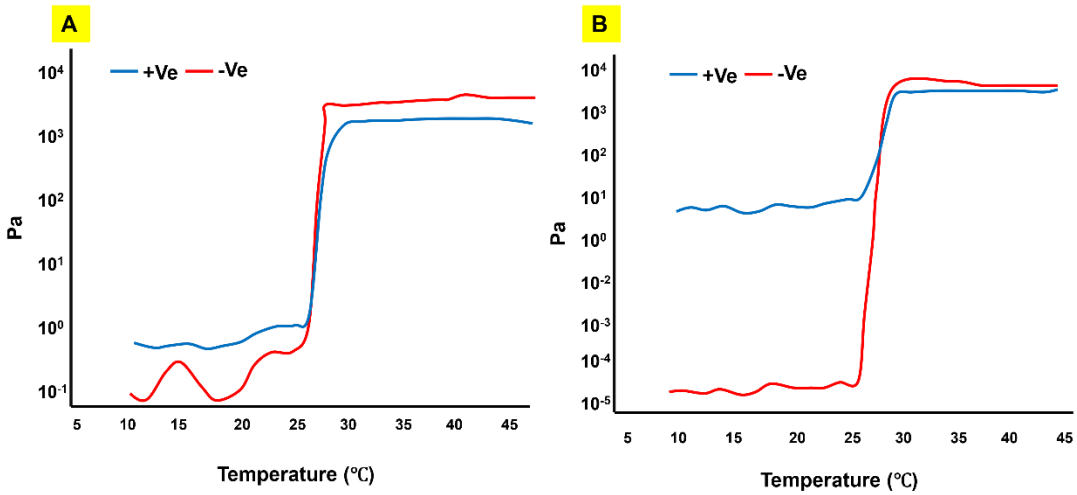

Fig. 14. The (+Ve) and (-Ve) values of PF127 hydrogel (A) and AuNPs-PF127 hydrogel (B) over a temperature range of 5 to 45 °C

Skin irritation test

When administered topically to mice, the AuNPs-PF127 hydrogel did not cause any negative effects such as skin redness, dryness, or desquamation. Both the PF127 hydrogel and AuNPs-PF127 hydrogel treated animals had normal skin conditions, indicating the hydrogel's skin compatibility (Fig.15).

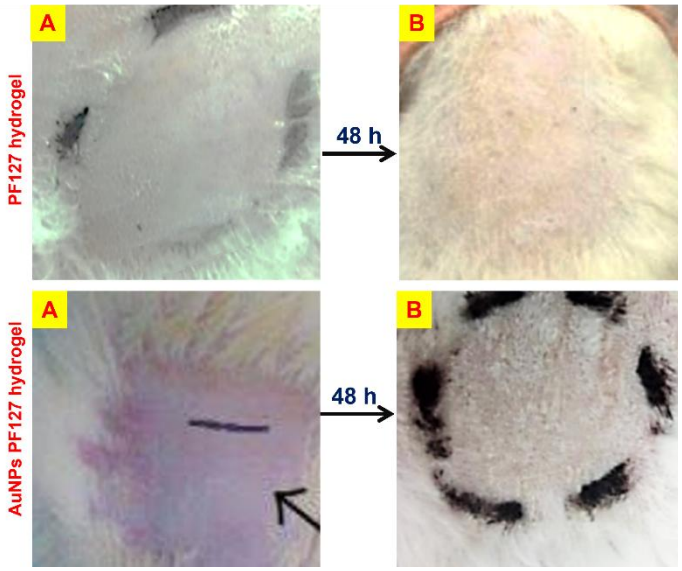

Fig. 15. Skin irritation test on both PF127 hydrogel alone and AuNPs PF127 hydrogel images after 48 h of treatment

Analysis of wound healing

The effectiveness of the healing process was evaluated by measuring the size of the wound on day 1 and its subsequent closure by day 10. The control group showed wound contraction percentages of 24.1%, 43.2%, 57.2%, and 61.2% on the day 3, day 5, day 7, and day 10, respectively.

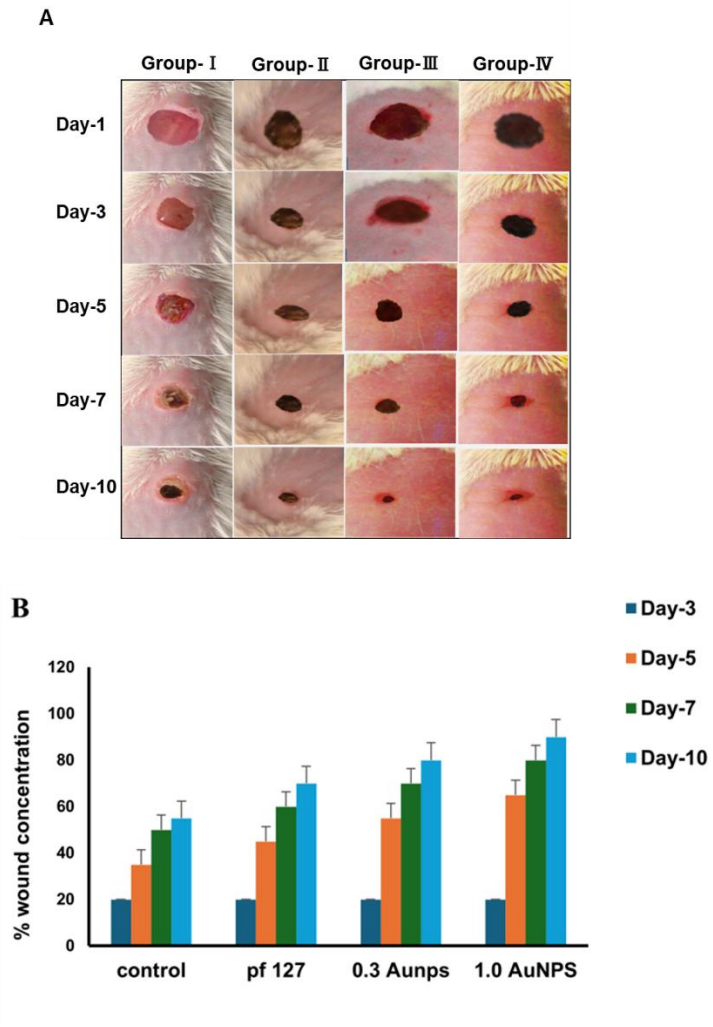

Fig. 16. Wound healing process in 4 groups of mice (A) and % of wound contraction (B)

Wounds treated with different hydrogels showed varying levels of contraction over time: pristine PF127 hydrogel contracted by 26.4%, 51.2%, 68.4%, and 76.7%; 0.3 mg AuNPs-PF127 hydrogel showed improvements of 27.2%, 52.3%, 75.4%, and 85.5%; and 1.0 mg AuNPs-PF127 hydrogel demonstrated the most significant healing rates of 24.2%, 56.4%, 85.2%, and 94.5% on the respective days. The study emphasised the exceptional healing properties of the 1.0 mg AuNPs-PF127 hydrogel, which almost completely closed wounds by the 10th day, indicating its potential as a successful wound healing treatment. In contrast, the wound healing rate of the AuNPs-PF127 hydrogel was faster than that of the group that used PF127 hydrogel alone (Fig. 16).

DISCUSSION

It has been reported that secondary metabolites in the *A. paniculata* extract, including polyphenols, flavonoids, alkaloids, polysaccharides, triterpenoids, as well as amino acids, vitamins, proteins, and other organic acids, may play a significant role in reducing and stabilizing generated particles in the synthesis of NPs via metal ion reduction (Maity *et al*. 2020). Among them, polyphenols and flavonoids may have contributed to the formation of AuNPs. There are numerous studies that have emphasized the role of Au NPs in wound healing (Vijayakumar *et al.* 2017; Satpathy *et al.* 2020). For example, Chen *et al.* created a combination of Au NPs and antioxidants

that significantly accelerates diabetic wound healing by modulating angiogenesis and providing anti-inflammatory effects (Chen *et al.* 2012). Consequently, the healing time for diabetic ulcers is significantly reduced. Furthermore, another team employed a sun-assisted hydrogel method to synthesize Au NPs, resulting in particles with optimal size, shape, and surface functionalization also exhibited antibacterial and wound-healing properties (Batool *et al* 2022).

AuNPs can be identified by a distinctive absorbance band, which is typically observed at a wavelength of 500 to 600 nm. This band is an outcome of the SPR phenomenon, which is dependent on the size of the nanoparticles. Electrons within metal nanoparticles collectively oscillate, causing SPR to resonate with light waves. Previous investigations have documented SPR bands for nanogold in the 530 to 550 nm range (Mujeeb *et al.* 2020; Noruzi 2015). The SPR peak for *A. paniculata* extract was in the 540 to 560 nm range in this study, suggesting that the extract is effective in the reduction of Au ions to AuNPs through bio-reduction processes. The biotransformation of metal ions to nanoparticles was observed to be both effective and rapid. A prominent band at 3474 cm^{-1} in the FTIR spectra, which corresponds to the stretching vibrations of OH groups that are commonly present in polyphenols, appears to be the driving force behind this bio-reduction process. FTIR confirmed the presence of O–H, C=C and C=O functional groups that contribute to the SPR observed in UV-Vis spectroscopy. Similarly, TEM combined with FTIR can give a comprehensive view of the surface characteristics and modifications. Both –OH and C=O groups from the *A. paniculata* extract not only reduced the Au^{3+} ions but also capped the nanoparticles, preventing aggregation and maintaining their stability and uniformity. Phytochemicals which exhibit comparable vibrational bands, have been implicated in the reduction of Au^{3+} in FTIR analyses from previous research (Ashwini and Mahalingam 2020; Hadi *et al* 2016). The XRD patterns of AuNPs synthesized from plant extracts frequently exhibit a prominent peak along the (111) plane, which indicates a preferred crystalline orientation. Similar XRD studies for other plant-mediated AuNPs production may be found (Khatua *et al*. 2020; Annamalai *et al*. 2013). The present data confirm the distribution of AuNPs, the similar AuNPs made through photosynthesis have been reported earlier (Shahriari *et al.* 2019; Gupta and Padmanabhan 2021).

The structural findings of other studies (Shahriari *et al* 2019; Gupta and Padmanabhan 2021; Hammami *et al.* 2021) were consistently supported by the TEM analysis of AuNPs in this research, which identified specific sizes and morphologies. The EDX examination of AuNPs revealed an optical absorption peak at around 2.2 keV (Elavazhagan and Arunachalam 2011). These results can be used to verify that the crystalline peaks observed in XRD correspond to AuNPs, ensuring that the sample is pure and free from other elements, also the results of EDX is correlates with the SPR peak observed in UV-Vis spectroscopy, thus validating the formation of AuNPs. The SAED data supports by the previous research (Gopinath *et al.* 2014) and the DLS data supports previous reports (Wacławek *et al.* 2018, Uzma *et al.* 2020), which suggest that the synthesized AuNPs are remarkably stable and remain within the nanometre range.

Various diseases, such as cancer, atherosclerosis, hypertension, and diabetes, are influenced by oxidative stress. The herbal plant *A. paniculata* is known for its potent antioxidant and anti-diabetic properties. Antioxidants, which are organic compounds, possess the ability to prevent or delay the oxidation of substrates, even at low concentrations (Al-Radadi 2022). Research has demonstrated that *A. paniculata* is abundant in antioxidants (Karpagasundari and Kulothungan 2014a,b). The ROS activity of AuNPs was assessed using the DPPH assay. The synthesised AuNPs at higher concentrations led to a significant increase in DPPH radical scavenging activity. Both the plant extract and AuNPs demonstrated peak radical scavenging efficiencies ranging from 86% to 90%. The antioxidant properties of synthesized AuNPs have yet

to be explored; however, similar plant-mediated synthesized AuNPs have demonstrated promising results (Veeramani *et al.* 2021; Ghosh *et al.* 2020). The antimicrobial activity of the synthesized AuNPs was assessed against clinically pertinent pathogens that are responsible for severe infections, underscoring the necessity of active therapeutic agents. The effectiveness was assessed by measuring the zone of inhibition surrounding the well after incubation. The nanoparticles produced using *A. paniculata* extracts had strong antibacterial characteristics, making them potential carriers for antibacterial agents. Furthermore, nanoparticles produce free radicals that interact with cellular proteins, lipids, and DNA, indicating that *A. paniculata*-mediated AuNPs possess substantial antimicrobial properties. Similarly, previous investigations have observed that biosynthesized AuNPs exhibit improved antimicrobial efficacy (Donga *et al.* 2020; Durga *et al.* 2020).

Diabetes is a worldwide health issue, and effective therapeutic alternatives are frequently derived from natural sources. Complications in the cardiovascular and nervous systems are associated with Type 2 Diabetes Mellitus (T2DM), which is defined by hyperglycaemia. The degradation of complex carbohydrates to glucose is facilitated by key enzymes such as alpha-glucosidase and alpha-amylase. Consequently, the inhibition of these enzymes is a prevalent therapeutic strategy for T2DM. In this study, the anti-diabetic effects of *A. paniculata* aqueous extract and synthesized AuNPs were compared using an alpha-amylase inhibition assay. The aqueous extract and the synthesized AuNPs both showed a substantial ability to block α -amylase enzyme activity, indicating a noteworthy anti-diabetic impact of 90 to 93%. Similar, studies on plant-mediated AuNPs and extracts have demonstrated potential (Banerjee *et al*. 2017; Veeramani *et al.* 2021).

Wound healing is a complex procedure that involves the formation of extracellular matrix, migration, and cell proliferation to reestablish the body's natural barrier to the external environment. Bacteria, including *S. aureus*, are likely to infect untreated incisions. The development of AuNP-based dressings for wound care has been promoted by the broad-spectrum antimicrobial properties of AuNPs. The present research has shown that AuNPs have the potential to disrupt bacterial cells and enhance their antioxidant capacity, rendering them an ideal choice for wound dressing applications. Plant-based dressings, including films, foams, and gels, are replacing conventional wound dressings like gauze, bandages, and plasters (Krishnan and Thomas 2019). The thermosensitivity of Pluronic polymers, or poloxamers, is particularly promising, as they will transition to a gel state at the body's physiological temperature of 37 °C. PF127, a biodegradable and biocompatible polymer with exceptional mechanical properties, is employed in drug delivery systems to treat cutaneous conditions and cancer (Akash and Rehman 2015; Chatterjee *et al.* 2019). The optimal filling and adhesion to the lesion area are guaranteed by the viscosity measurement of gel preparations for topical applications (Mekkawy *et al.* 2013).

The viscosity of the AuNPs-PF127 hydrogel was comparable to that of PF127 alone, suggesting that the gel's flow properties were not affected by the AuNPs' inclusion. The ideal formulation enabled uniform epidermal coverage, with a spreadability that ranged from 6.0 to 7.7 cm (El-Kased *et al*. 2017). Furthermore, AuNPs-PF127 hydrogel did not induce skin irritation in rodents, which corroborates its potential for wound treatment. To restore the functionality of epidermis and tissues that have been damaged, wound healing is a dynamic process that necessitates the coordinated activity of a variety of biochemical elements (Diegelmann and Evans 2004). The potential of the PF127 hydrogel as an optimal wound dressing is underscored by the controlled release of AuNPs and the synergistic action of AuNPs. The small particle size increases the surface area to volume ratio, enhancing the interaction with microbial cells and promoting better antimicrobial activity (Rajakannu

et al. 2015; Gupta *et al.* 2024). When treating lesions with chemically synthesized nanoparticles in gelatine hydrogels, Diniz *et al.* (2020) observed that the healing process typically takes more than 14 days. The present findings were particularly noteworthy, as they demonstrated an accelerated healing process, with complete healing occurring within 10 days of treatment with AuNPs-PF127 hydrogel. The sustained release of AuNPs was responsible for the accelerated healing, as it enabled them to interact with inflammatory cells at the lesion site without causing damage to healthy cells. In summary, our research has shown that green-synthesized AuNPs can be more effective in terms of their antibacterial and antioxidant properties, as well as their prolonged efficacy.

CONCLUSIONS

1. Gold nanoparticles (AuNPs) produced with usage of the herb *A. paniculata* have been confirmed suitable for biomedical uses through multiple characterisation analyses.
2. The particles exhibited an average size of 23 nm, and their stability was confirmed by zeta potential experiments. The anisotropic characteristics of these AuNPs, in terms of their form and size, were clearly shown in UV-Vis spectra and confirmed through TEM imaging.
3. The AuNPs produced from *A. paniculata* showed impressive antidiabetic, antioxidant, antibacterial, and wound healing effects. Their significant role in wound healing was demonstrated by the closure of incisions within 10 days, showcasing their potential in managing wounds.
4. The addition of these AuNPs to PF127 hydrogel increased the rate of wound contraction in mice without causing skin irritation. This biosynthesized AuNPs-loaded hydrogel is a feasible and environmentally friendly option for treating bacterial infections and promoting wound healing.
5. These findings support the use of AuNPs as a highly effective drug delivery technology with broad applications in nano biopharmaceutical and biomedical fields, highlighting its contribution to developing environmentally friendly and efficient therapeutic solutions.

ACKNOWLEGMENTS

This work was supported by National Natural Science Foundation of China [81873332].

Data Availability

The data associated with the findings of this study are available from the corresponding authors, upon reasonable request.

Conflict of Interest

Authors have declared that no conflict of interest is associated with this work.

REFERENCES CITED

Akbar, S. (2011). "*Andrographis paniculata*: A review of pharmacological activities and clinical effects," *Alternative Medicine Review* 16(1), 66-77.

Akintelu, S. A., Yao, B., and Folorunso, A. S. (2021). "Green synthesis, characterization, and antibacterial investigation of synthesized gold nanoparticles (AuNPs) from *Garcinia kola* pulp extract," *Plasmonics* 16, 157-165 (2021). DOI: 10.1007/s11468-020-01274-9

Al-Bayaty, F. H., Abdulla, M. A., Hassan, M. I. A., and Ali, H. M. (2012). "Effect of *Andrographis paniculata* leaf extract on wound healing in rats," *Natural Product Research* 26(5), 423-429. DOI: 10.1080/14786419.2010.496114.

Al-Dahmash, N. D., Al-Ansari, M. M., Al-Otibi, F. O., and Singh, A. J. A. R. (2021). "Frankincense, an aromatic medicinal exudate of *Boswellia carterii* used to mediate silver nanoparticle synthesis: Evaluation of bacterial molecular inhibition and its pathway," *J. Drug Delivery Sci. Technol.* 61, article 102337. DOI: org/10.1016/j.jddst.2021.102337

Allafchian, A., Balali, F., Reza., Vahabi, M., and AmirHosseinJalali, S. (2022). "Antibacterial and cytotoxic efects of silver nanoparticles fabricated by *Eryngium billarderi* Delar," *Extract. Chem. Phys. Lett.* 791, article 139385. DOI: 10.1016/j.cplett.2022.139385

Al-Radadi, N. S. (2022). "Biogenic proficient synthesis of (Au-NPs) via aqueous extract of red dragon pulp and seed oil: Characterization, antioxidant, cytotoxic properties, anti-diabetic anti-inflammatory, anti-Alzheimer and their antiproliferative potential against cancer cell lines," *Saudi J. Biol. Sci.* 29(4). DOI: 10.1016/j.sjbs.2022.01.001

Ajaya, R., Sridevi, K., Kumar, V. N., Nanduri, S., and Rajagopal, S. (2004). "Anticancer and immunostimulatory compounds from *Andrographis paniculata*," *Journal of Ethnopharmacology* 92, 291-295.

Akash, M. S. H., and Rehman, K. (2015). "Recent progress in biomedical applications of Pluronic (PF127): Pharmaceutical perspectives," *J. Control. Release* 209, 120-138. DOI: 10.1016/j.jconrel.2015.04.032

Anand, U., Jacobo-Herrera, N., Altemimi, A., and Lakhssassi, N. (2019). "A comprehensive review on medicinal plants as antimicrobial therapeutics: Potential avenues of biocompatible drug discovery," *Metabolites* 9, article 258. DOI: 10. 3390/metabo9110258

Annamalai, A., Christina, V. L. P., Sudha, D., Kalpana, M., and Lakshmi, P. T. V. (2013). "Green synthesis, characterization and antimicrobial activity of AuNPs using *Euphorbia hirta* L. leaf extract," *Colloids Surf. B Biointerfaces* 108, 60-65. DOI: 10.1016/j.colsurfb.2013.02.012

Arafa, M. G., El-Kased, R. F., and Elmazar, M. M. (2018). "Thermoresponsive gels containing gold nanoparticles as smart antibacterial and wound healing agents," *Sci. Rep.* 8, article 13674. DOI: 10.1038/s41598-018-31895-4

Arunachalam, K. D., and Annamalai, S. K. (2013). "Chrysopogon zizanioides aqueous extract mediated synthesis, characterization of crystalline silver and gold nanoparticles for biomedical applications," *International Journal of Nanomedicine* 8, 2375-2384. DOI: 10.2147/IJN.S44076

Ashwini, D., and Mahalingam, G. (2020). "Green synthesized metal nanoparticles, characterization and its anti-diabetic activities – A review," *Res. J. Pharm. Technol.* 13, 468-474. DOI: 10.5958/0974-360X.2020.00091.8.

Bapat, R. A., Chaubal, T. V., Dharmadhikari, S., Abdulla, A. M., Bapat, P., Alexander, A., Dubey, S. K., and Kesharwani, P. (2020). "Recent advances of gold nanoparticles as biomaterial in dentistry," *Int. J. Pharm*. 586, article 119596.

DOI: 10.1016/j.ijpharm.2020. 119596

Batool, Z., Muhammad, G., Iqbal, M. M. *et al.* (2022). "Hydrogel assisted synthesis of gold nanoparticles with enhanced microbicidal and in vivo wound healing potential," *Sci. Rep.* 12, article 6575. DOI: 10.1038/s41598-022-10495-3

Benabderrahim, M. A., Yahia, Y., Bettaieb, I., Elfalleh, W., and Nagaz. K. (2019). "Antioxidant activity and phenolic profile of a collection of medicinal plants from Tunisian arid and Saharan regions," *Ind. Crops Prod*. 138, article 111427.

Banerjee, A., Maji, B., Mukherjee, S., Chaudhuri, K., and Seal, T. (2017). "Green synthesis of gold NPs using sumac aqueous extract and their antioxidant activity," *Int. J. Curr. Pharm. Res.* 9. DOI: 10.5101/NBE.V8I1.P1-8

Calabrese, C., Berman, S. H., Babish, J. G., Ma, X., Shinto, L., Dorr, M., and Standish, L. J. (2000). "A phase I trial of andrographolide in HIV positive patients and normal volunteers," Bastyr University Research Institute, Bastyr University, Washington 98028 USA. Phytotherapy Research, 14, 333-338.

Chen, L.X., He, H., Xia, G. Y., Zhou, K. L., and Qiu, F. (2014). "A new flavonoid from the aerial parts of *Andrographis paniculata*," *Natural Product Research*. 28(3), 138-143. DOI: 10.1080/14786419.2013.856907

Chen, S. A., Chen, H. M., Yao, Y. D., Hung, C. F., Tu, C. S., and Liang, Y. J. (2012). "Topical treatment with antioxidants and Au nanoparticles promotes healing of diabetic wound through receptor for advance glycation end-products," *Eur. J. Pharm. Sci.* 47, article 875.

Chatterjee, S., Hui, P. C., Kan, C., and Wang, W. (2019). Dual-responsive (pH/temperature) Pluronic F-127 hydrogel drug delivery system for textilebased transdermal therapy," *Sci. Rep*. 9, article 11658. DOI: 10.1038/s41598-019-4

Dao, M. U., Le, H. S., Hoang, H. Y., Tran, V. A., Doan, V. D., Le, T. T. N., and Sirotkin, A. (2021). "Natural core-shell structure activated carbon beads derived from *Litsea glutinosa* seeds for removal of methylene blue: Facile preparation, characterization, and adsorption properties," *Environ. Res*. 198, article 110481.

Diegelmann, R. F., and Evans, M. C. (2004). "Wound healing: An overview of acute, fibrotic and delayed healing," *Front. Biosci*. 9, 283-289. DOI: 10.2741/ 1184

Diniz, F. R., Maia, R., Rannier, L., Andrade, L. N., Chaud, V., da Silva, M., *et al.* (2020). "Silver nanoparticles-composing alginate/gelatine hydrogel improves wound healing in vivo," *Nanomaterials* 10, article 390. DOI: 10.3390/nano100 20390

Donga, S., Bhadu, G. R., and Chanda, S. (2020). "Antimicrobial, antioxidant and anticancer activities of gold nanoparticles green synthesized using *Mangifera indica* seed aqueous extract," *Artif. Cells Nanomed. Biotechnol*. 48(1). DOI: 10.1080/21691401.2020.1843470.

Durga, B., Julius, A., Pavithradevi, S., and Sumaya Fathima, A. R. (2020). "Study of phytochemical constituents and antibacterial activity of methanol extract of *Physalis minima* Linn," *Eur. J. Mol. Clin. Med*.

Elahi, N., Kamali, M., and Baghersad, M. H. (2018). "Recent biomedical applications of gold NPs a review," *Talanta* 184, 537-556. DOI: 10.1016/j.talanta.2018.02.088

Elavazhagan, T., and Arunachalam, K. D. (2011). "*Memecylon edule* leaf extract mediated green synthesis of silver and gold nanoparticles," *Int. J. Nanomed.* 6, 1265-1278. DOI: 10.2147/IJN.S18347

El-Houssieny, B. M., and Hamouda, H. M. (2010). "Formulation and evaluation of clotrimazole from pluronic F127 gels," *Drug Discov. Ther.* 4, 33-43.

El-Kased, R. F., Amer, R. I., Attia, D., and Elmazar, M. M. (2017). "Honey-based hydrogel: In vitro and comparative in vivo evaluation for burn wound healing," *Sci. Rep*. 7, article 9692. DOI: 10.1038/s41598-017-08771-8

Guo, L., Jackman, J. A., Yang, H. H., Chen, P., Cho, N. J., and Kim, D. H. (2015). "Strategies for enhancing the sensitivity of plasmonic nanosensors," *Nano Today*

10(2), 213-239. DOI: 10.1016/j.nantod.2015.02.007

Gupta, R., and Padmanabhan, P. (2021). "Biogenic synthesis and characterization of gold nanoparticles by a novel marine bacteria marinobacter algicola: Progression from nanospheres to various geometrical shapes," *Biotechnol. Sci. F* 732-737. DOI: 10.15414/jmbfs.2018.8.1.732-737

Gupta, S., Choudhary, D. K., and Sundaram, S. (2024). "Green synthesis and characterization of silver nanoparticles using *Citrus sinensis* (orange peel) extract and their antidiabetic, antioxidant, antimicrobial and anticancer activity," *Waste Biomass Valor*. DOI: 10.1007/s12649-024-02782-z

Ghosh, N. S., Pandey, E., Giilhotra, R. M., and Singh, R. (2020). "Biosynthesis of gold NPs using leaf extract of *Desmodium gangeticum* and their antioxidant activity," *Res. J. Pharm. Technol*. 13, 2685-2689. DOI: 10.5958/0974-360x.2020.00477.1

Ghosh Chaudhuri, R., and Paria, S. (2022). "Core/shell nanoparticles: classes, properties, synthesis mechanisms, characterization, and applications," *Chem Rev*. 112, 2373-2433.

Hammami, I., Alabdallah, N. M., Al jomaa, A., and Kamoun, M. (2021). "Gold nanoparticles: Synthesis properties and applications," *J. King Saud Univ. – Sci*. 33(7), article 101560. DOI: 10.1016/j.jksus.2022.101989.

Huang, H., Qi, X., Chen, Y., and Wu, Z. (2019). "Thermo-sensitive hydrogels for delivering biotherapeutic molecules: A review," *Saudi Pharma. J*. 27, 990-999. DOI: 10.1016/j.jsps.2019.08.001

Kabir, M., Hasan, N., Rahman, M., Khan, J. K., Hoque, N. T., Bhuiyan, M. R. Q., Mou, S. M., Jahan, R., and Rahamatullah, M. (2014). "A survey of medicinal plants used by the Deb barma clan of the Tripura tribe of Moulvibazar district, Bangladesh," *Journal of Ethnobiology and Ethnomedicine* 10(1), article 19. DOI: 10.1186/1746-4269-10-19

Karpagasundari, C. S., and Kulothungan. (2014). "Analysis of bioactive compounds in *Physalis minima* leaves using GC MS, HPLC, UV-VIS and FTIR techniques," *J. Pharmacog. Phytochem*. 3(4), 196-201.

Kalimuthu, K., Cha, B. S., Kim, S., and Park, K. S. (2020). "Eco-friendly synthesis and biomedical applications of gold nanoparticles: A review," *Microchem. J*. 152, article 104296. DOI: 10.1016/j.microc.2019.104296

Khatua A., Priyadarshini E., Rajamani P., Patel A., Kumar J., Naik A., *et al*. (2020). "Phytosynthesis, characterization and fungicidal potential of emerging gold nanoparticles using *Pongamia pinnata* leave extract: A novel approach in nanoparticle synthesis," 31(1), 125-131. DOI: 10.1007/S10876-019- 01624-6.

Kifle, Z. D., and Enyew, E. F. (2022). "Evaluation of in vivo antidiabetic, in vitro a-amylase inhibitory, and in vitro antioxidant activity of leaves crude extract and solvent fractions of *Bersama abyssinica* Fresen (Melianthaceae)," *J. Evid. Based Integr. Med*. 25. DOI: 10.1177/2515690X20935827.

Krishnan, K. A., and Thomas, S. (2019). "Recent advances on herb-derived constituents-incorporated wound-dressing materials: A review," *Polym. Adv. Technol.* 30, 823-838. DOI: 10.1002/pat.4540

Kumar, R. A., Sridevi, K., Kumar, N. V., Nanduri, S., and Rajagopal, S. (2004). "Anticancer and immunostimulatory compounds from *Andrographis paniculata*," *Journal of Ethnopharmacology* 92(2-3), 291-295. DOI: 10.1016/j.jep.2004.03.004

Lee, K. X., Shameli, K., Yew, Y. P., Teow, S. Y., Jahangirian, H., RajeeMoghaddam, R., and Webster, T. J. (2020). "Recent development in the facile biosynthesis of Gold NPs (Au-NPs) and their biomedical applications," *Int. J. Nanomedicine*. 15, 275. DOI: 10.2147/IJN.S233789

Martin, A. (1996). "The use of antioxidants in wound healing," *Dermatologic Surgery* 22, 156-160.

Mekkawy, A., Fathy, M., and El-Shanawany, S. (2013). "Formulation and in vitro evaluation of fluconazole topical gels," *Br. J. Pharm. Res*. 3, 293-313.

Mohamad, N., Mohd Amin, M. C., Pandey, M., Ahmad, N., and Rajab, N. F. (2014). "Bacterial cellulose/acrylic acid hydrogel synthesized via electron beam irradiation: Accelerated burn wound healing in an animal model," *Carbohydr. Polym.* 114, 312-320. DOI: 10.1016/j.carbpol.2014.08.025

Nguyen, T. H. A., Nguyen, V. C., Phan, T. N. H., Vasseghian, Y., Trubitsyn, M. A., Nguyen, A. T., and Doan, V. D. (2022). "Novel biogenic silver and gold nanoparticles for multifunctional applications: Green synthesis, catalytic and antibacterial activity, and colorimetric detection of Fe (III) ions," *Chemosphere* 287.

Noruzi, M. (2015). "Biosynthesis of gold nanoparticles using plant extracts," *Bioprocess Biosyst. Eng*. 38(1), 1-14. DOI: 10.1007/s00449-014-1251-0

Niska, K., Zielinska, E., Radomski, M. W., and Stepniak, I. (2018). "Metal nanoparticles in dermatology and cosmetology: Interactions with human skin cells," *Chemico-Biological Interactions* 295, 38-51. DOI: 10.1016/j.cbi.2017.06.018

Nurhaslina, C. R., Mealianny, Mustapa, A. N., and Mohd Azizi, C. Y. (2019). "Total phenolic content, flavonoid concentration and antioxidant activity of indigenous herbs *Physalis minima* Linn.," *J. Phys.: Conf. Ser.* 1349, 1-7. DOI: 10.1088/ 1742-6596%2F1349%2F1%2F012088.

Nyabola, A. O., Kareru, P. G., Madivoli, E. S., Wanakai, S. I., and Maina, E. G. (2020). "Formation of silver nanoparticles via *Aspilia pluriseta* extracts their antimicrobial and catalytic activity," *Journal of Inorganic and Organometallic Polymers and Materials* 30(9), article 34. DOI: 10.1007/s10904-020-01497-7

Owaid, M. N., Rabeea, M. A., Aziz, A. A., Jameel, M. S., and Dheyab, M. A. (2019). "Mushroom assisted synthesis of triangle gold nanoparticles using the aqueous extract of fresh *Lentinula edodes* (shiitake), Omphalotaceae," *Environ. Nanotechnol*. 12, article 100270.

Patil, K. B., Patil, N. B., Patil, S. V., Patil, V. K., and Shirsath, P. C. (2020). "Metal based nanomaterials (silver and gold) synthesis and biomedical applications," *Asian J. Pharm. Technol.* 10, 97-106. DOI: 10.5958/2231-5713.2020.00018.5

Maity, G. N., Maity, P., Choudhuri, I., Sahoo, G. C., Maity, N., Ghosh., K., Bhattacharyya, N., Dalai, S., and Mondal, S. (2020). "Green synthesis, characterization, antimicrobial and cytotoxic effect of silver nanoparticles using arabinoxylan isolated from Kalmegh" *International Journal of Biological Macromolecules*, 162, 1025–1034. DOI: 10.1016/j.ijbiomac.2020.06.215

Mehrishi, P., Agarwal, P., Broor, S., and Sharma, A. (2020). "Antibacterial and antibiofilm properties of medicinal plant extracts against multi drug resistant *Staphylococcus* species and nonfermenter bacteria," *J. Pure Appl. Microbiol.* 14(1), 403-413. DOI: 10.22207/JPAM.14.1.42

Qiao, J., and Qi, L. (2021). "Recent progress in plant-gold nanoparticles fabrication methodsand bioapplications," *Talanta* 223, article 121396. DOI: 10.1016/j.talanta. 2020.121396

Rajakannu, Subashini & Shankar, Sruthi & Pethaperumal, Sindhuja & Subramanian, Santhini & Dhakshinamoorthy, Gnana. (2015). "Biosynthesis of silver nanoparticles using *Garcinia mangostana* fruit extract and their antibacterial, antioxidant activity," *International Journal of Current Microbiology and Applied Sciences* 4. 944-952.

Raymond, J. T., and Hamidreza, K. (2024). "Structural and antimicrobial properties of synthesized gold nanoparticles using biological and chemical approaches," *Front. Chem. Sec. Nanoscience* 12, article 1482102. DOI: 10.3389/fchem.2024.1482102

Satpathy, S., Patra, A., Ahirwar, B., and Hussain, M. D. (2020). "Process optimization for green synthesis of gold nanoparticles mediated by extract of *Hygrophila spinosa* T. Anders and their biological applications," *Phys. E: Low. -Dimens. Syst. Nanostruct*. 121, article 113830.

Shanmugam, R., Balusamy, S. R., Kumar, V., Menon, S., Lakshmi, T., and Penumalsamy, H. (2020). "Biosynthesis of gold nanoparticles using marine microbe (*Vibrio alginolyticus*) and its anticancer and antioxidant analysis," *J. King Saud Univ. Sci.* 33(1), article 10. DOI: 10.1016/j.jksus.2020.101260

Shahriari, M., Hemmati, S., Zangeneh, A., and Zangeneh, M. M. (2019). "Biosynthesis of gold nanoparticles using *Allium noeanum* Reut. ex Regel leaves aqueous extract characterization and analysis of their cytotoxicity, antioxidant, and antibacterial properties," *Appl. Organomet. Chem*. 33(11), article e5189.

Sheeja, K., Shihab, P. K., and Kuttan, G. (2006). "Antioxidant and anti-inflammatory activities of the plant *Andrographis paniculata* Nees," *Immunopharmacology Immunotoxicology* 28, 129-140.

Shukla, A., Rasik, A. M., and Dhawan, B. N. (1999). "Asiaticoside-induced elevation of antioxidant levels in healing wounds," *Phytotherapy Research* 13, 50-54.

Shanwaz, M. M., and Shyam, P. (2023). "Anti-bacterial effect and characteristics of gold nanoparticles (AuNps) formed with *Vitex negundo* plant extract," *Appl. Biochem. Biotechnol.* 195, 1630-1643 (2023). DOI: 10.1007/s12010-022-04217-8

Singha, P. K, Roy, S., and Dey, S. (2003). "Antimicrobial activity of *Andrographis paniculata*," *Fitoterapia* 74, 692-694.

Siddiqi, K. S., and Husen, A. (2017). "Recent advances in plant-mediated engineered gold NPs and their application in biological system," *J. Trace Elem. Med. Biol*. 40, 10-23. DOI: 10.1016/j.jtemb.2016.11.012

Siddiqi, K. S., Husen, A., and Rao, R. A. K. (2018). "A review on biosynthesis of silver nanoparticles and their biocidal properties," *Journal of Nanobiotechnology* 16(1), 14-18. DOI: 10.1186/s12951-018-0334-5

Tripathi, R., and Kamat, J. P. (2007). "Free radical induced damages to rat liver subcellular organelles: Inhibition by *A. paniculata* extract," *Indian Journal of Experimental Biology* 45, 959-567.

Trivedi, N. P., and Rawal, U.M. (2001). "Hepatoprotective and antioxidant property of *Andrographis paniculata* Nees in BHC induced liver damage in mice," *Indian Journal of Experimental Biology* 39, 41-46.

Unayana, N., Uzma, M., Dhanwini, R. P., Govindappa, M., Prakash, H. S., and Vinay Raghavendra, B. (2020). "Green synthesis of gold nanoparticles from *Vitex negundo* leaf extract to inhibit lipopolysaccharide-induced inflammation through in vitro and in vivo," *J. Clust. Sci.* 31(2), 463-477.

Uzma, M., Sunayana, N., Raghavendra, V. B., Madhu, C.S., Shanmuganathan, R., and Brindhadevi, K. (2020). "Biogenic synthesis of gold nanoparticles using *Commiphora wightii* and their cytotoxic effects on breast cancer cell line (MCF-7)," *Process Biochem*. 92, 269-276. DOI: 10.1016/j. procbio.2020.01.019

Veeramani, S., Narayanan, A. P., Yuvaraj, K., Sivaramakrishnan, R., Pugazhendhi, A., Rishivarathan, I., Jose, S. P., and Ilangovan, R. (2021). "*Nigella sativa* flavonoids surface coated gold NPs (Au-NPs) enhancing antioxidant and anti-diabetic activity," *Process Biochem*. 114, 193-202. DOI: 10.1016/J.PROCBIO.2021.01.004.

Vijayakumar, V., Samal, S. K., Mohanty, S., and Nayak, S. K. (2019). "Recent advancements in biopolymer and metal nanoparticlebased materials in diabetic wound healing management," *International Journal of Biological Macromolecules* 122, 137-148. DOI: 10.1016/j.ijbiomac.2018.10.120

Vijayakumar, S., Vaseeharan, B., Malaikozhundan, B., Gopi, N., Ekambaram, P.,

Pachaiappan, R., and Suriyanarayanamoorthy, M. (2017). "Therapeutic effects of gold nanoparticles synthesized using *Musa paradisiaca* peel extract against multiple antibiotic resistant *Enterococcus faecalis* biofilms and human lung cancer cells (A549)," *Microb. Pathog*. 102, 173-183. DOI: 10.1016/j.micpath.2016.11.029.

Wacławek, S., Gončuková, Z., Adach, K., Fijałkowski, M., and Černík, M. (2018). "Green synthesis of gold nanoparticles using *Artemisia dracunculus* extract: Control of the shape and size by varying synthesis conditions," *Environ. Sci. Pollut. Res. Int.* 25 (24), 24210-24219. DOI: 10.1007/s11356-018-2510-4.

Article submitted: September 30, 2024; Peer review completed: October 26, 2024; Revised version received: December 20, 2024; Accepted: December 22, 2024; Published: February 17, 2025.
DOI: 10.15376/biores.20.2.2687-2710